



## Investigation of vehicle exhaust sub-23 nm particle emissions

B. Giechaskiel, J. Vanhanen, M. Väkevä & G. Martini

To cite this article: B. Giechaskiel, J. Vanhanen, M. Väkevä & G. Martini (2017) Investigation of vehicle exhaust sub-23 nm particle emissions, *Aerosol Science and Technology*, 51:5, 626-641, DOI: [10.1080/02786826.2017.1286291](https://doi.org/10.1080/02786826.2017.1286291)

To link to this article: <https://doi.org/10.1080/02786826.2017.1286291>



© 2017 European Union. Published with license by American Association for Aerosol Research© European Union



Accepted author version posted online: 25 Jan 2017.  
Published online: 08 Feb 2017.



Submit your article to this journal [↗](#)



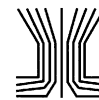
Article views: 896



View Crossmark data [↗](#)



Citing articles: 6 View citing articles [↗](#)



## Investigation of vehicle exhaust sub-23 nm particle emissions

B. Giechaskiel<sup>a</sup>, J. Vanhanen<sup>b</sup>, M. Väkevä<sup>b</sup>, and G. Martini<sup>a</sup>

<sup>a</sup>Sustainable Transport Unit, Institute for Energy, Transport and Climate, Joint Research Centre, European Commission, Ispra, Italy; <sup>b</sup>AirmodusOy, Helsinki, Finland

### ABSTRACT

A solid particle number limit was applied to the European legislation for diesel vehicles in 2011. Extension to gasoline direct injection vehicles raised concerns because many studies found particles below the lower size limit of the method (23 nm). Here we investigated experimentally the feasibility of lowering this size. A nano condensation nucleus counter system (nCNC) ( $d_{50\%} = 1.3$  nm) was used in parallel with condensation particle counters (CPCs) ( $d_{50\%} = 3$  nm, 10 nm and 23 nm) at various sampling systems based on ejector or rotating disk diluters and having thermal pre-treatment systems consisting of evaporation tubes or catalytic strippers. An engine exhaust particle sizer (EEPS) measured the particle size distributions. Depending on the losses and thermal pre-treatment of the sampling system, differences of up to 150% could be seen on the final detected particle concentrations when including the particles smaller than 23 nm in diameter. A volatile artefact as particles with diameters below 10 nm was at times observed during the cold start measurements of a 2-stroke moped. The diesel vehicles equipped with the Diesel Particulate Filter (DPF) had a low solid sub-23 nm particles fraction (<20%), the gasoline with direct injection vehicles had higher (35–50%), the gasoline vehicles with port fuel injection and the two mopeds (two and four-stroke) had the majority of particles below 23 nm. The size distributions peaked at 60–80 nm for the DPF equipped vehicles, at 40–90 nm for the gasoline vehicles with a separate nucleation mode peak at approximately 10 nm sometimes. Mopeds peaked at sizes below 50 nm when their aerosol was thermally pre-treated.

### ARTICLE HISTORY

Received 20 October 2016  
Accepted 16 January 2017

### EDITOR

Matti Maricq



### Introduction

The Solid Particle Number (SPN) standard was introduced in the European Union legislation for diesel light-duty vehicles in September 2011 (Euro 5b), limiting the number of solid particles emitted during the legislated test cycle to  $6 \times 10^{11}$  p/km. The new standard effectively necessitated the installation of high-efficient wall-flow diesel particulate filters (DPFs) in all light-duty diesel vehicles. The SPN standard was also introduced for heavy-duty engines used in on-road applications in 2013 (Euro VI). The same standard was introduced for gasoline vehicles utilizing direct injection (G-DI) at Euro 6 stage (September 2014) initially with a limit of  $6 \times 10^{12}$  p/km and from September 2017 with  $6 \times 10^{11}$  p/km. A SPN limit will also be introduced in the Non-Road Mobile Machinery engines regulation at Stage V (from 2017).

The SPN method is based on the findings of the Particle Measurement Program (PMP; Andersson et al. 2007; Giechaskiel et al. 2008). Exhaust gas enters a volatile

particle remover (VPR), which consists of a hot diluter ( $>150^\circ\text{C}$ ) and an evaporation tube (ET) at  $350^\circ\text{C}$  followed by a diluter at ambient temperature. At the exit of the VPR, a condensation particle counter (CPC) measures particles  $>23$  nm (50% cut-point). In this article, particles after thermal pre-treatment at approximately  $350^\circ\text{C}$  are called 'solid' by convention.

There were concerns whether the methodology applied to diesel engines could be applied to gasoline engines and other technologies. A literature survey showed that solid nucleation mode of particles  $<23$  nm can be emitted and sometimes in high concentrations (Giechaskiel et al. 2014). Summarizing the review, a lot of studies have found a solid nucleation mode with older and modern diesel engines, both at low and high loads (Kittelson et al. 2006; Rönkkö et al. 2007). Solid nucleation mode was often observed at gasoline engines with port fuel injection (G-PFI) and it was assumed to originate from the metals of the lube oil or from fuel additives

**CONTACT** B. Giechaskiel  [Barouch.Giechaskiel@ec.europa.eu](mailto:Barouch.Giechaskiel@ec.europa.eu)  Sustainable Transport Unit, Institute for Energy, Transport and Climate, Joint Research Centre, European Commission, Via E. Fermi 2749, Ispra, VA I-21027, Italy.

Color versions of one or more of the figures in the article can be found online at [www.tandfonline.com/uast](http://www.tandfonline.com/uast).

© 2017 European Union

This is an Open Access article. Non-commercial re-use, distribution, and reproduction in any medium, provided the original work is properly attributed, cited, and is not altered, transformed, or built upon in any way, is permitted. The moral rights of the named author(s) have been asserted.

Published with license by American Association for Aerosol Research

(Mayer et al. 2010; Gidney et al. 2010). At G-DI vehicles a small solid nucleation mode at 10–20 nm appeared quite often in the size distribution (Khalek et al. 2010; Szybist et al. 2011; Ntziachristos et al. 2013) but also during decelerations conducted by engine braking (Rönkkö et al. 2014; Karjalainen et al. 2014). The percentage of solid particles not measured (i.e., <23 nm) during a test cycle has been reported to be on average 30–40% without considering the particle loss in the sampling system (Giechaskiel et al. 2014). Higher percentages were measured at low ambient temperatures or high ethanol fuels. It should be mentioned that in some studies it was recognized that the measured ‘solid’ nucleation mode was a (volatile) re-nucleation artefact downstream from the evaporation tube (Johnson et al. 2009; Zheng et al. 2011, 2012). Re-nucleation downstream from the evaporation tube has been shown when sulfur (Swanson et al. 2009) and/or ammonia is available (Amanatidis et al. 2014). When the concentration of hydrocarbons is sufficient, these particles grow to sizes detectable with commonly used instruments (around 7–10 nm) (see, e.g., summary in Giechaskiel and Martini 2014) and in some cases >23 nm (Zheng et al. 2014; Giechaskiel et al. 2016). It should be clarified at this point that in general, volatile particles are not an artefact in real exhaust; they can sometimes dominate the particle number (PN) emissions as a separate nucleation mode (Kittelson 1998; Keskinen and Rönkkö 2010). Volatiles condensed on soot particles are also part of the Particulate Matter (PM) as measured with the gravimetric method. Here, we consider them as an artefact only when they appear after the thermal pre-treatment of the SPN measurement system.

The emissions of sub-23 nm particles have been gaining a lot of attention over the last few years. There are mainly two reasons: (1) sub-23 nm particles might be more harmful to human health than bigger particles as they have higher deposition efficiency in the respiratory system and can translocate to other areas such as the brain (Oberdörster et al. 2004); (2) the fraction is not negligible for vehicles not equipped with a DPF (Giechaskiel et al. 2014). However, once emitted small nanoparticles are transformed into bigger particles by coagulation processes. Thus, due to their lower residence time in the atmosphere, the sub-23 nm particles should have fewer possibilities to be inhaled. Nevertheless, it should be kept in mind that the diluted exhaust gas can reach citizens in a few seconds/minutes at busy roads.

Researchers around the world are evaluating the possibility of reducing the lower size limit of the measurement systems without affecting the measurement uncertainty and reproducibility (Herner et al. 2007; Zheng et al. 2012; Yamada et al. 2015). In the PMP

group, there are ongoing discussions on the possibility of reducing the lower particle size below 23 nm for the future World Harmonized Light Duty legislation (Giechaskiel and Martini 2014). A Horizon 2020 call for ‘Technologies for low emission light-duty powertrains’ was launched with special emphasis on the sub-23 nm particle measurements (Horizon 2020). There are three groups that will investigate the topic in great detail: DownToTen, Soreal-23, PEMS4Nano.

The current understanding of the feasibility of solid sub-23 nm particle measurements for regulatory purposes was summarized in the review paper by Giechaskiel and Martini (2014). Lowering the cut-off size of the SPN system to 3 nm can often lead to wrong results due to the re-nucleation downstream from the VPR with an evaporation tube (i.e., measuring volatiles as solid particles): This could happen when the soot surface is low (e.g., with particulate filters; Zheng et al. 2012), during regeneration (high exhaust gas temperatures; Giechaskiel et al. 2016) or when the concentration of organics is high (e.g., mopeds; Giechaskiel et al. 2015b). The re-nucleated particles are usually small in size and do not grow more than 10 nm when the dilution is high enough (typically, the primary dilution around 100 or higher; Yamada et al. 2015). However, high dilution is not required by the regulation; only a hot primary dilution is required, and that the CPC measures in its single particle count range. In addition, the solid particle losses of existing commercial VPRs increase significantly with a decreasing size and typically exceed 50% at 10 nm. For sub-10 nm measurements the final result is very sensitive to the sampling setup (e.g., length of hoses, flow rates, etc.) due to particle losses. Thus, so far, it seems feasible to lower the lower size to around 10 nm without significantly affecting the measurement uncertainty and without introducing artefacts, but not lower (Giechaskiel and Martini 2014). Lowering the 50% cut-point of existing CPCs to 10 nm is relatively easy and can be achieved simply with software modifications and re-calibration. For measurements of particles >10 nm, according to Giechaskiel and Martini (2014), a catalytic stripper (CS; Khalek and Kittelson 1995; Amanatidis et al. 2012; Otsuki et al. 2014) in place or in addition to the Evaporation Tube (ET) is recommended to ensure that hydrocarbons are oxidized and that no volatile re-nucleated particles will grow at the 10 nm range. The thermodenuder was not excluded, but there are studies that have in some cases shown formation of solid particles (Swanson and Kittelson 2010). At this point, it should also be mentioned that SPN measurements of >10 nm (50% cut-off) will be introduced in the aviation sector (Lobo et al. 2015). The particle losses in the sampling and conditioning system will be corrected based on

an estimation of the mean particle size from the non-volatile mass and SPN measurements.

Although the 10 nm lower particle size limit would cover the majority of the cases, it would probably leave some vehicles that emit very small particles uncovered (Alanen et al. 2015). Combustion studies have shown that nanoparticles in the range of 1–5 nm are formed in large concentrations (D'Anna 2009). Some studies have found solid nucleation mode below 10 nm for heavy-duty diesel (Rönkkö et al. 2007) or G-DI (Khalek et al. 2010) engines. To our knowledge, only one study has measured below 3 nm (Alanen et al. 2015). The reported losses in the particle measurement system for the 3 nm range were >65% and the results typically have high uncertainty.

Although solid particles above or below 23 nm are of high interest for regulatory purposes, total PN emissions and size distributions from the dilution tunnel are under investigation in the United States to provide an alternative to the regulated mass method, which has reached its detection limit in modern vehicles equipped with a DPF (Liu et al. 2009). Total particle concentrations are the focus of atmospheric studies as well (see, e.g., review of Morawska et al. 2008). In addition, special attention is given to the fresh nucleation mode, which peaks at around 20 nm and is mainly attributed to traffic; vehicles contribute up to 90% on busy roads (Kumar et al. 2014). In the laboratory, specific conditions that favour nucleation mode and mimic ambient conditions can reproduce the concentration of the nucleation mode (within a factor of 2–10) formed on the road at the tailpipe of vehicles relatively well (see, e.g., review of Keskinen and Rönkkö 2010). However, these tests were conducted with a porous type diluter directly at the tailpipe of a vehicle and not in the dilution tunnel.

The primary objective of this article is to investigate the capabilities of commercial systems for sub-23 nm SPN measurements. Special attention is given to the sub-10 nm range where existing systems have high uncertainty. This is achieved by using different sampling systems, CPCs with different cut-points and the nCNC (>1 nm).

Based on the data collected for the characterization of the sampling systems, the fractions of solid sub-23 nm particles of two diesel vehicles equipped with a DPF, four gasoline vehicles (two G-PFI and two G-DI) and two mopeds (2-stroke and 4-stroke) are also presented. The results are also compared with literature. Total PN concentrations, i.e., concentrations of all particles, including volatile ones, and size distributions are also presented.

## Experimental

The experiments were conducted with 8 different vehicles, using several different dilution and conditioning (sampling) systems and different particle counting technologies.

### Vehicles used

The vehicles that were tested are presented in Table 1. Diesel vehicles were equipped with DPFs and Diesel Oxidation Catalysts. Two of the gasoline vehicles were with Port Fuel Injection (G-PFI) and two with Direct Injection (G-DI), both equipped with a Three-Way-Catalyst. The two mopeds with Continuously Variable Transmission (CVT) were 2-stroke and 4-stroke, respectively.

The vehicles were tested with the corresponding type approval cycle: the New European Driving Cycle (NEDC) for light-duty vehicles and the UNECE Regulation 47 cycle (R47) for mopeds. Details for the cycles can be found elsewhere: e.g., Dieselnets (2016) and Giechaskiel et al. (2015b). For the Euro 6 gasoline vehicles the future type approval World Harmonized Light Duty Test Cycle (WLTC) was used (GTR15 2016; Ciuffo 2015). In addition, a few future type approval World Harmonized Motorcycle Transient Cycles (WMTC) and steady state cycles were conducted with the mopeds. Fuels were reference fuels with 5% biodiesel (B5) or 5% or 10% ethanol (E5, E10). Lube oils were those from the manufacturers; the composition is unknown. Semi-synthetic lube oil was used for the mopeds. For the 2-stroke moped 2% of lube oil was mixed to the fuel.

**Table 1.** Characteristics of test vehicles.

Vehicle ID	Engine and aftertreatment technology	Engine capacity [cm <sup>3</sup> ]	Emission limit	Rated power [kW]	Odometer [km]	Fuels	Cycles
DPF_1	Diesel, Diesel Oxidation Catalyst, Diesel particulate Filter	3000	6B	190	7200	B5	NEDC
DPF_2	Diesel, Diesel Oxidation Catalyst, Diesel particulate Filter	2000	6B	160	27200	B5	NEDC
G-PFI_1	Gasoline, Port-Fuel Injection, Three-Way-Catalyst	1600	5	75	57100	E5	NEDC
G-PFI_2	Gasoline, Port-Fuel Injection, Three-Way-Catalyst	1400	6B	57	7800	E5	WLTC
G-DI_1	Gasoline, Direct Injection, Three-Way-Catalyst	1200	5	63	7000	E5	NEDC
G-DI_2	Gasoline, Direct Injection, Three-Way-Catalyst	1600	6B	140	20000	E10	WLTC
Mo_2s	Moped, gasoline, 4-stroke, CVT, carburettor, two-way-catalyst	50	2	2	<500	E5	R47, steady
Mo_4s	Moped, gasoline, 2-stroke, CVT, carburettor, two-way-cat	50	2	2	<500	E5	R47, WMTC, steady

## Description of emission measurement systems

The experimental setup is presented in Figure 1. All systems were connected to the full dilution tunnel with a constant volume sampler (CVS) (hereinafter, the terms dilution tunnel and CVS are used interchangeably). Particulate matter (PM) mass was measured on a filter sampling 50 l/min from the CVS (TX40 Teflon-coated glass-fiber filter) according to the regulation (temperature at the filter  $<52^{\circ}\text{C}$ ). Tests were conducted with CPCs of different 50% cut-points and a nano condensation nucleus counter (nCNC) connected to an AVL particle counter with a catalytic stripper (APC/CS) for the measurement of solid particles. A dual ejector system with an evaporation tube (EJ/ET) was used for a limited number of tests in place of the APC/CS to investigate the effect of the sampling system on the measured concentrations. The nCNC was also connected to the CVS for a few tests to measure the total PN  $> 1$  nm. An engine exhaust particle sizer (EEPS) connected to the CVS tunnel measured particle size distributions. The EEPS was used for a limited number of tests with a CS or a thermodenuder (TD) to measure solid particles. The description of the systems follows.

The APC (AVL Particle Counter 489; Giechaskiel et al. 2010) is compliant with Regulation 83 (2015) for light-duty vehicles that measures solid particles. The system consists of a hot rotating disk dilution at  $150^{\circ}\text{C}$ , an ET at  $350^{\circ}\text{C}$  and a secondary porous tube dilution at ambient temperature. The APC/CS is the APC with a CS downstream from the ET (before the secondary dilution). The specific CS was evaluated by Amanatidis et al. (2012). It has an oxidation efficiency of  $>99\%$  of decane, and a sulfur trap with sulfur capacity of  $>6$  mg (as measured with  $\text{SO}_2$ ).

For most tests, CPCs with 50% counting efficiency at 23 nm (TSI 3790), 10 nm (TSI 3771) and 3 nm (TSI

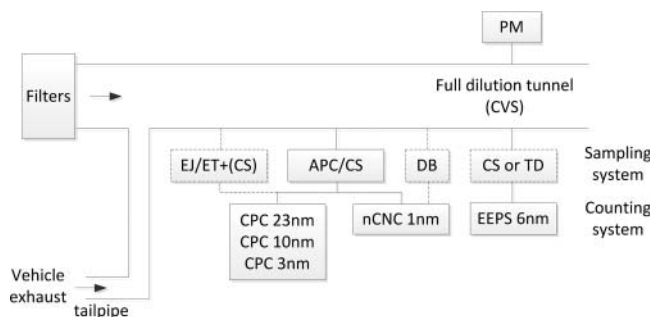


**Figure 1.** Experimental setup. Dashed lines indicate optional parts. APC = AVL particle counter; CPC = condensation particle counter; CS = catalytic stripper; CVS = constant volume sampler; DB = dilution bridge; EJ = ejector; ET = evaporation tube; nCNC = nano condensation nucleus counter; TD = thermodenuder.

3025A) were connected to this system (Tuch et al. 2016). The 23 nm CPC was connected with a 40 cm ( $d_{in} = 4$  mm, flow rate 1 l/min, 2.5% particle losses at 23 nm) silicon conductive tubing, while the 10 nm and the 3 nm CPC with a 10 cm ( $d_{in} = 4$  mm, flow rate 1 l/min, 2.5% particle losses at 10 nm) and 40 cm ( $d_{in} = 4$  mm, flow rate 1.5 l/min, 5% particle losses at 10 nm and 20% at 3 nm) tubes respectively from the exit of the APC.

For some tests, a dual ejector dilution system was used in place of the APC/CS. In the dual ejector system (EJ/ET; Dekati), the first dilution was conducted with a heated EJ (dilution air  $150^{\circ}\text{C}$  and blanket  $150^{\circ}\text{C}$ ; Giechaskiel et al. 2009). The diluted sample was further heated in an ET ( $350^{\circ}\text{C}$ ) and then further diluted by a secondary EJ at ambient temperature.

Particle size distributions from 5.6 to 560 nm with a sizing resolution of 16 channels per decade (a total of 32 channels) were measured with an EEPS (TSI Engine Exhaust Particle Sizer Spectrometer 3090). At the instrument's inlet, there is a cyclone with a 50% cut-size at  $1 \mu\text{m}$  (inlet flowrate 10 lpm). By integrating the size distribution, the total PN concentration was estimated. As the instrument was directly connected to the CVS, it was considered that it measured volatile and non-volatile particles of  $>6$  nm (called total PN by convention) with a 1.5 m ( $d_{in} = 6$  mm) conductive silicone tube. For a few tests with mopeds, a CS from AVL (Amanatidis et al. 2012) at  $300^{\circ}\text{C}$  or a high flow (10 l/min) thermodenuder (Dekati) were used to remove the volatile particles. Their 50% penetration was around 10 nm. The difference in concentration between the EEPS and the 23 nm CPC in their common size range was between 20–25% (EEPS measuring higher). This difference (20%) was corrected in our results. The calibration details can be found in Giechaskiel et al. (2015a). The recently-introduced inversion 'soot' algorithm that was designed for fractal particles was used (Wang et al. 2016). We should also add that the nucleation mode measured by the EEPS is sometimes underestimated (Xue et al. 2015).

The AirmodusnCNC (Airmodus A11 nano Condensation Nucleus Counter) measures PN concentrations starting from approximately 1 nm in diameter. It is a combination of a particle size magnifier (PSM) and an Airmodus butanol CPC. The PSM is used to grow particles and clusters that are below the detection limit of the butanol CPC (5 nm) to detectable sizes (Vanhanen et al. 2011). The PSM grows the particles by mixing the sample turbulently with particle-free air heated and saturated with diethylene glycol (DEG). This rapid mixing activates and grows the particles by condensation of DEG up to about 90 nm in electrical mobility diameter (Vanhanen et al. 2011). Mixing type design allows the user to change the mixing ratio and thus the lowest



detection limit of the instrument. In this study, the instrument was used in its lowest detection limit setting, giving the nCNC system a cut-off diameter of about 1.3 nm (calibrated with tungsten oxide particles). The cut-off diameter for any measurement technology that is based on growing the aerosol particles with condensable vapours is dependent on the composition of the particles and the vapour that is used (Mamakos et al. 2013). The effect of particle composition and, for example, charge when studying sub-3 nm particles is discussed elsewhere (Kangasluoma et al. 2014, Lahtipalo et al. 2016). While the cut-off diameter for tungsten oxide is 1.3 nm, it can be closer to 2 nm for organic compounds with the same instrument settings. Due to internal losses inside the PSM and the CPC, the maximum detection limit at plateau height is about 80% (as calibrated with NaCl particles by the manufacturer). The instrument was connected to the sampling system (APC/CS or ET/EJ+DB) or directly to the CVS (without dilution or through the DB) with a 40 cm silicon conductive hose ( $d_{in} = 4\text{ mm}$ , 4% particle losses at 10 nm, 15% at 3 nm for 2.5 l/min). The results in this study were corrected only by 20% to take the losses of the system at the plateau region into account, unless otherwise specified.

### Particle losses inside the sampling systems

We measured the aerosol penetration ratios for the APC/CS and EJ/ET systems using silver particles up to 50 nm produced with the evaporation-condensation method in  $N_2$ . We also thermally pre-treated them in a catalytic stripper at 375°C in order to make them spherical (Ku and Maynard 2006).

We also calibrated the EJ/ET system with graphite particles produced with a spark-discharge particle generator (PALAS DNP 3000) at sizes 15, 30, 50 and 100 nm. Particles were thermally pre-treated in a CS at 375°C in order to have the same setup as with silver particles. The APC/CS was calibrated with soot-like particles (from propane diffusion flame AVL APG 499) by the manufacturer at 15, 30, 50, and 100 nm.

Penetration curves following the correction with the mean particle number concentration reduction factor (PCRf) of 30, 50, and 100 nm, as required by the legislation, are presented in Figure 2. The PCRf at a specific size is the ratio of the upstream and downstream concentrations when measuring mono-disperse aerosol of the specific size. Thus, the mean PCRf is basically the total dilution of the system including the particle losses as average losses at 30, 50, and 100 nm. This means that the number concentration of size distributions with geometric mean diameters (GMDs) around 50 nm is measured correctly (within 10%), because the mean PCRf is

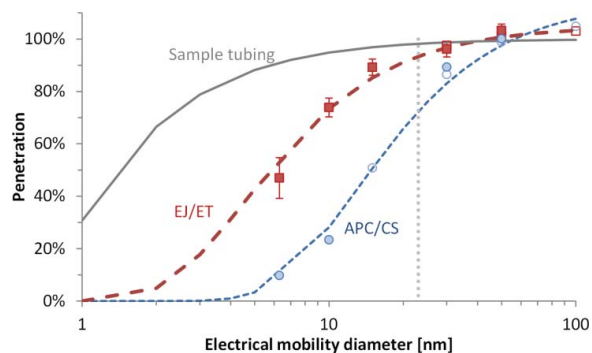


**Figure 2.** Penetration curves following the correction with the mean PCRf (average of 30, 50, 100 nm). Symbols are experimental data. ‘Sample tubing’ refers to a hose of 40 cm length, inner diameter of 4 mm and flow rate of 1.5 l/min. Dashed lines are only there to help the eye. Open symbols are soot-like particles (propane diffusion flame for APC/CS and spark-discharged graphite for EJ/ET), while solid symbols are silver particles. Error bars indicate min-max of two measurements on different days.

optimized for sizes around 50 nm. The penetration efficiencies at 100 nm are slightly higher than 100% and for this reason the PN concentration of size distributions with GMDs of >100 nm is overestimated. The PN concentration of size distributions with GMDs of <30 nm are underestimated (Giechaskiel et al. 2012; Giechaskiel and Martini 2014). This will be addressed in the Results section, but in general, the results of size distributions that peak at around 10–20 nm would need a correction of a factor of up to 2, depending on the system.

The penetration efficiency through sampling tubing between the sampling system and the counting instruments is also given as a function of a particle size in Figure 2 based on the diffusion loss equations (Gormley and Kennedy, 1949). Error bars are given only for the EJ/ET system with silver particles based on measurements on two different days. The measurements have an uncertainty of <5% at sizes  $\geq 30$  nm and 5–10% (in absolute levels) for smaller sizes.

As presented in Figure 2, the penetrations of systems at 10 nm are between 25% and 75%. Although we have no experimental data, extending the penetration curves based on diffusion losses of long tubes, we assume that only the EJ/ET has a penetration of >15% at 3 nm. This means that any sub-3 nm particles can be distinguished only by the EJ+DB system. For the APC/CS, the nCNC (>1 nm) is expected to measure equally with the 3025A (3 nm) even if there are sub-3 nm particles present.

Losses for the sub-30 nm particle in the sampling systems and sampling lines were not taken into account (i.e., the results presented in this article were corrected only with the 30, 50, and 100 nm mean PCRf), but the effect will be discussed in the results section.

## Background concentration levels of the measurement systems

Background levels were measured for the whole systems consisting of the dilution, evaporation and the particle counting instrument. Typically, background levels of the systems are determined by measuring HEPA filtered air at their inlet before any measurement. According to the Regulation 83 (2015), the particle concentration must be  $<0.5 \text{ p/cm}^3$  (without PCRF/dilution correction) for the 23 nm CPCs. Such levels or lower were measured with all CPCs (23 nm, 10 nm, 3 nm). For the nCNC ( $>1 \text{ nm}$ ), the background was on average around  $3 \text{ p/cm}^3$ , but spikes could reach  $10 \text{ p/cm}^3$ . Probably this is because Particle Size Magnifier is tuned so close to homogeneous nucleation threshold and thus, for example, humidity and temperature changes create some background (Vanhanen, 2011).

It should be noted that for some systems, background levels of  $>1 \text{ nm}$  (but not with the rest of the CPCs) were  $>100 \text{ p/cm}^3$  (up to  $2000 \text{ p/cm}^3$  in one case). Our assumption for those 1–3 nm particles is that they are formed from deposited materials (contaminants) inside the evaporation tube and/or the cold dilution stage. Another explanation is that this background is due to heavy hydrocarbons from the dilution air, which are not captured by the filter. The nCNC would also detect clusters, i.e., clusters of molecules that might penetrate the HEPA filter. The results of these systems are not discussed in this article. However, we assume that systems with high sub-3 nm background are more susceptible to nucleation when sulfur containing volatile material is available.

## Volatile removal efficiency

Volatile removal efficiency was tested with monodisperse tetracontane particles as prescribed in the legislation. All systems could remove  $10^4 \text{ p/cm}^3$  of 30 nm tetracontane particles. Tests with polydisperse aerosol of GMD  $>100 \text{ nm}$  (concentration  $>10^6 \text{ p/cm}^3$ ) also showed efficiencies of  $>99\%$  for the APC/CS and CS, but not for the standalone TD (Giechaskiel et al. 2009, 2015a).

## Results and discussion

### Volatile artefact

We evaluated the volatile artefact, i.e., formation of volatile nucleation particles downstream of the evaporation tube that are counted as ‘solid’ particles, by comparing the ‘solid’ emissions of a system with the total emissions for the specific vehicle.

We conducted a test with a 2-stroke moped with the EJ/ET+DB system, where we measured emissions of  $>400$  times higher than the rest of the systems (even higher than the EEPS that measures total particle concentration) when particles  $<23 \text{ nm}$  were considered (figure not shown). Placing a CS downstream from the second diluter removed this volatile nucleation mode. These results confirm the findings of other studies (Giechaskiel et al. 2015b; Zheng et al. 2012) that volatile artefact below 23 nm is possible with evaporation tubes and for this reason we recommend a catalytic stripper (as discussed in Giechaskiel and Martini 2014).

The use of catalytic strippers needs attention. Volatile artefact of  $<10 \text{ nm}$  was also noticed in a few cases with the 2-stroke moped even when using the APC/CS. Figure 3 shows emissions measured at the beginning of the R47 cycle with different instruments. The GMD at the beginning of the cycle was  $>200 \text{ nm}$  (mass  $>50 \text{ mg/m}^3$ ). It was confirmed that there were no particles of diameter  $<6 \text{ nm}$  by measuring with the nCNC at the CVS: EEPS and nCNC measured similar concentrations (within the experimental uncertainties of the EEPS and the repeatability on different days). Concentrations of  $>10 \text{ nm}$  following thermal pre-treatment were close to the CVS levels. However,  $>3 \text{ nm}$  concentrations at the beginning of the cycle were higher than the CVS emissions, indicating a volatile artefact even downstream from the CS. This could be due to inefficient evaporation of volatile precursors in the evaporation tube upstream from the CS and, consequently, reduced oxidation efficiency of the CS (Amanatidis et al. 2012) or formation of sulfur particles due to  $\text{SO}_2$  to  $\text{SO}_3$  conversion in the CS (Amanatidis et al. 2012). The last explanation is highly unlikely at the temperature where the CS was operated, but it's something that requires investigation. The PCRF of the APC/CS

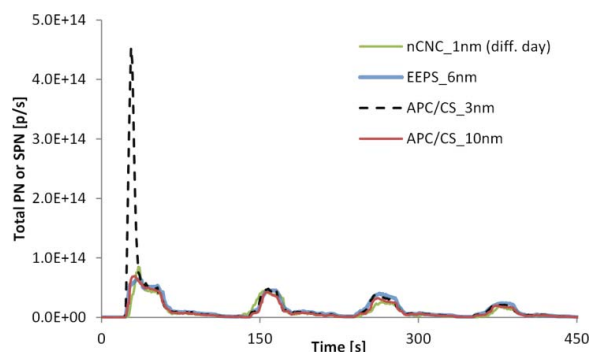


**Figure 3.** Real-time measurements in the cold start part of the R47 with the 2-stroke moped using E5 fuel (Mo\_2s). EEPS and nCNC were measuring total PN, while the APC/CS was measuring SPN.

was  $100 \times 10$  (primary, secondary dilution), and the concentration of the CPC reached  $90,000 \text{ p/cm}^3$  compared to the rest of the instruments, which measured on the order of  $10,000 \text{ p/cm}^3$ . Although  $90,000 \text{ p/cm}^3$  is still within the measurement range of the specific CPC (3025A), the full flow CPCs usually measure up to  $10,000 \text{ p/cm}^3$  in single particle count mode as required in the legislation. Thus, this test would be identified as non-valid.

Volatile artefact was also noticed when the EEPS was used with the thermodenuder at the CVS. Even with dilution ratio up to 50:1, a nucleation mode could be seen. At dilution ratio 250:1, it disappeared (or it shrunk below the detection limit of the EEPS due to the high dilution used).

Volatile artefact of the PMP systems has already been discussed in literature especially for sub-23 nm particle measurements (Zheng et al. 2012; Mamakos et al. 2013; Giechaskiel et al. 2015b). Recently artefacts for sizes  $>23 \text{ nm}$  have been reported: during the cold start of 2-stroke moped (Giechaskiel et al. 2015b), during the regeneration of heavy-duty vehicle using low PCRF (Giechaskiel et al. 2016) and during on-road tests with a heavy duty diesel truck driving uphill (Zheng et al. 2014).

Our results demonstrate and confirm the difficulty of measuring 'true' solid particles below 10 nm, confirming the conclusion of Giechaskiel and Martini (2014). The key message of these tests is that future regulations have to better define the volatile removal efficiency requirements (or capabilities) of the emission measurement systems. The case examined here is extreme: There was 2% lubricant in the fuel and the exhaust aerosol of 2-stroke engines includes unburnt fuel and lubricant. 2-stroke engines do not have any SPN limit and until 2020, only a feasibility study is foreseen (Giechaskiel et al. 2015b). In addition, they tend to phase out due to the stringent Euro 4 and 5 limits for L-category vehicles. Nevertheless, the capabilities of the sampling systems should be well-known: The systems should be capable of removing the semi-volatile particle emissions of the applications studied when investigating solid particles of  $<10 \text{ nm}$ . For example in the review of Giechaskiel and Martini (2014) nucleation mode with mass up to  $1.5 \text{ mg/m}^3$  at the CVS has been reported for diesel vehicles, but it can be much higher when no catalyst is used. Mopeds can exceed  $50 \text{ mg/m}^3$  at cold start (Giechaskiel et al. 2015b). During a regeneration of a heavy duty diesel vehicle mass of approximately  $0.5 \text{ mg/m}^3$  was measured in the CVS (Giechaskiel et al. 2016). At the moment the volatile removal efficiency requirement is  $>1 \times 10^4 \text{ p/cm}^3$  of particles 30 nm, which covers a very low mass ( $0.1 \text{ } \mu\text{g/m}^3$ ). Our proposal is to define a higher size and/or concentrations of the test material (tetracontane) in order to check

mass  $>1 \text{ mg/m}^3$ . This mass can be reached for example with polydisperse aerosol with size  $>50 \text{ nm}$  and concentration of  $1 \times 10^7 \text{ p/cm}^3$ . This mass can cover most of the cases that would be encountered. The efficiency should be checked with the lowest size measuring instrument that will be used in tests.

### Effect of the sampling system's penetration on the final results

In order to investigate the effect of the sampling system on the final result of the sub-23 nm particle emission levels, R47 cycles were performed with a 4-stroke moped using the CPCs and the nCNC connected either at the APC/CS or the EJ/ET. Figure 4a (cold part R47: first four sub-cycles) and Figure 4b (hot part R47: last four sub-cycles) show the SPN emission levels as they were measured by different instruments connected to the APC/CS or EJ/ET systems (corrected with the mean PCRF of 30 nm, 50 nm, and 100 nm). The number concentrations of the sub-23 nm particles were in addition corrected

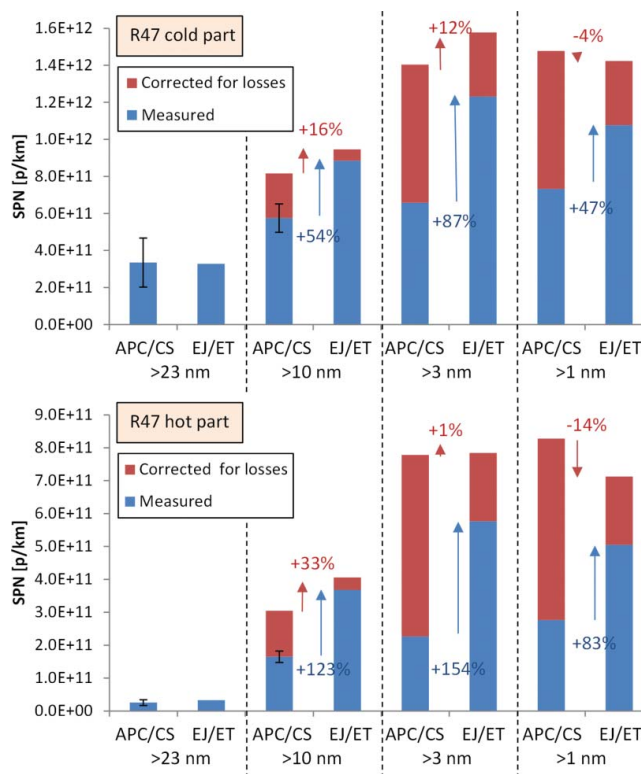


**Figure 4.** Emission levels of the 4-stroke moped as determined by different instruments for (a) cold part of the R47 cycle (first four sub-cycles) and (b) hot part of the R47 cycle (last 4 sub-cycles). Error bars show the variability of five tests conducted on different days. Only one test was available for the EJ/ET system and with the 3 nm CPC and the 1 nm nCNC. Arrows show the percentage differences between the two systems for uncorrected or corrected loss concentrations. Details of the corrections presented in the text.



with the penetration of each size range: 50% APC/CS and 90% EJ/ET for the 10–23 nm range, 10% APC/CS and 50% EJ/ET for the 3–10 nm range. As the 3 nm CPC and the 1 nm nCNC measured the same concentrations we assumed that, whether or not any existed in the diluted exhaust gas, no particles <3 nm penetrated the sampling system.

Focusing on the results without particle loss corrections, the measured number concentrations with the 10 nm and 3 nm CPCs are higher when the EJ/ET system is used instead of the APC/CS. Although for the >23 nm particles the differences between the two sampling systems are negligible, the difference of the two systems almost doubles for the smaller particles (the EJ/ET measured +54% to +87% for the cold part R47 and +83% to 154% for the hot part R47 compared to the APC/CS). By correcting the losses based on the penetration efficiencies, the differences decrease to <33% for all size ranges. Thus, it can be assumed that the main reason for the differences observed between the APC/CS and the EJ/ET was the different level of particle losses.

Another reason that can result in differences between sampling systems are the differences in volatile removal resulting in a different size of particles and, consequently, losses in the systems and counting efficiency in the counters. Finally, re-nucleation downstream from the evaporation tube as discussed in the section above can result in big differences.

Comparing measurements performed with systems with different penetration curves needs attention. Giechaskiel and Martini (2014) mentioned that the same average (of 30, 50, 100 nm) PCRF could be used even when the systems are modified to measure from 10 nm in order to keep the link with past measurements. They showed theoretically that this approach could work for the typically encountered size distributions with GMDs >40 nm. The suggested method could, however, lead to big differences (>50%) when the sub-23 nm particle fraction is high, as in the example of Figure 4. Yamada et al. (2015), who used a 3 nm CPC as the particle counter, reported that a better accuracy was achieved by including the losses of <23 nm particles as the PCRF of 15 nm in the mean PCRF. In the aviation sector, an aerosol particle mean size is calculated based on mass and number measurements, and an appropriate mean loss correction is then applied.

There are not many sampling systems with high volatile removal efficiency and low particle losses. To our knowledge, only the thermodenuder in the studies of Heikkilä et al. (2009) and Alanen et al. (2015) has high penetrations for the measurement of solid sub-10 nm particles (33–68% penetration for 3 to 10 nm diameter particles). We also assume that the system

of Khalek (2007) with a catalytic stripper would also have high penetration efficiencies at the sub-10 nm range, based on the presented >10 nm penetration curve. Proper design of thermodenuders (Fierz et al. 2007; Mendes et al. 2016) or catalytic stripper-based systems (Khalek 2007) can result in high penetrations, but at the moment we are not aware of any commercially available systems.

### **PM, total PN, and SPN emissions**

Table 2 presents PM mass, total PN and SPN emission levels for the examined vehicles. In general the PM mass and SPN emission levels are in agreement with the literature and a detailed discussion is out of the scope of this article (Maricq et al. 2002; Braiser et al. 2010; Mamakos et al. 2012; Giechaskiel et al. 2012; Kim et al. 2013; Zhu et al. 2016). The correlation of PM mass and SPN >23 nm (not considering the 2-stroke moped) gives a slope of  $0.9 \times 10^{12}$  p/mg which is at the low end of the reported slopes (typically  $1\text{--}4 \times 10^{12}$  p/mg, see review Giechaskiel et al. 2012; Zheng et al. 2014) indicating smaller produced mean particle sizes or higher density. Considering also the sub-23 nm particles, the correlation would change to  $1.5 \times 10^{12}$  p/mg. The PM of the 2-stroke moped consists of high percentage of volatiles due to high scavenging losses, and the addition of the lubricant in the combustion chamber (Ntziachristos et al. 2003). In our case, based on the PN measurements the non-volatile PM fraction is estimated to be only 25%. Using only the non-volatile part of the PM the 2-stroke moped would fall in the typical correlation values of PM-SPN.

### **Sub-23 nm fraction of solid particles**

Table 2 presents the percentage of particles below a specific size. In this section the emissions of solid particles will be discussed and in particular the sub-23 nm fractions. As the nCNC and the 3 nm CPC number concentrations were within 15% for the 2-stroke moped and 4-stroke moped, and the 1–3 nm particle penetration through the measurement systems is expected to be very low even with the EJ/ET system, no distinction is made in the table for the 1–3 nm range.

The SPN emissions of vehicles equipped with a DPF were low ( $<1 \times 10^{11}$  p/km), and the 10–23 nm and 1–10 nm percentages were also low <20%. The 1–10 nm percentage is not reported as the concentrations were close to the background level of the nCNC ( $3 \text{ p/cm}^3$ ).

Only one test was available with the G-PFI\_1 vehicle, and the SPN percentage of 10–23 nm fraction was 148%. This high percentage indicates that the

mean particle size is around 23 nm. However, in absolute levels the emissions are very low ( $0.77 \times 10^{11}$  p/km). For the other G\_PFI\_2 vehicle the percentage was lower (74%), but the absolute emissions higher ( $2.1 \times 10^{10}$  p/km). The G-DIs had emissions higher than the future limit for G-DI vehicles ( $6 \times 10^{11}$  p/km) but lower than the current limit for G-DIs until 2017 ( $6 \times 10^{12}$  p/km). Both the 10–23 nm and the 1–10 nm fractions were lower than 50%.

Regarding the 2-stroke moped, the percentage of particles below 23 nm is almost two times higher than the >23 nm emissions. The sub-10 nm fraction is 150%. The 4-stroke moped has sub-23 nm and sub-10 nm percentages of 70%. At steady states (no figure shown), the 10–23 nm fractions are even higher (see also Giechaskiel et al. 2015b, sub-23 nm particle fractions of mopeds and motorcycles).

In general, the percentages in Table 2 are in accordance with the results of Giechaskiel et al. (2014) and Giechaskiel and Martini (2015) plotted in Figure 5 for particles of >10 nm. Note that the percentages of Figure 5 are not corrected with the sub-23 nm losses; applying the correction would increase the sub-23 nm concentrations approximately 100% (Giechaskiel et al. 2014) (e.g., 46% would be 92%). Note also that in many cases, these percentages would be higher if particles of <10 nm were considered.

The DPFs are very efficient also at sizes between 10–23 nm, in accordance with other researchers that have shown higher filtration efficiency for smaller particles (Heikkilä et al. 2009). High concentrations of solid sub-23 nm particles have been measured with diesel engines without aftertreatment devices or low efficiency filters (Kittelson et al. 2006; Rönkkö et al. 2007; Heikkilä et al. 2009), but with high efficiency filters they usually disappear (Lähde et al. 2009). Particles can be formed by urea injection, and high sub-23 nm percentages can be measured (100%), but in

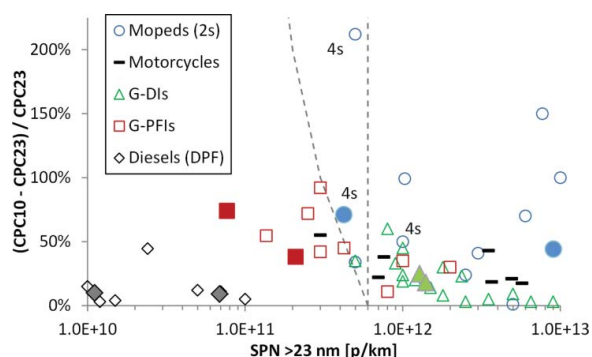


**Figure 5.** Reported sub-23 nm fraction of solid particles for different vehicles (from Giechaskiel and Martini 2015) as estimated by the differences of the 10 nm and 23 nm condensation particle counters (CPCs) of APC or APC/CS systems. Every point is an average of many tests with a specific vehicle, typically with the future type approval cycles. Solid (and bigger) symbols are the results of this study. All sub-23 nm fractions in this figure haven't been corrected for losses (i.e., a factor between 1.7 and 2 would be needed, depending on the system used). Vertical dashed line indicates the current limit of  $6 \times 10^{11}$  p/km for particles >23 nm in diameter. The other line indicates the same limit for particles >10 nm in diameter. All mopeds were 2-stroke unless otherwise specified in the figure.

absolute levels the concentration is low (Amanatidis et al. 2014; Giechaskiel et al. 2016).

G-DI vehicles have sub-23 nm percentages on the order of <50%. These percentages are in agreement with Khalek et al. (2010) and Mamakos et al. (2013). G-PFIs have higher sub-23 nm fraction but lower emissions in absolute levels. Other researchers have found high percentages of sub-23 nm particles (Gidney et al. 2010; Mayer et al. 2010, 2012). Alanen et al. (2015) measured high concentration of solid sub-10 nm particles downstream from a thermodenuder with a 1999 gasoline engine using natural gas. The percentages depend on the mean size of the produced particles, which depends on the combustion process; thus engine cold start, low

**Table 2.** PM mass, total PN, SPN emissions and their sub-23 nm particle fractions. The number after the instrument (EEPS, CPC, nCNC) gives the 50% cut-point that was used for the calculations (1, 6, 10, or 23 nm). The APC/CS sub-23 and sub-10 nm fractions have been corrected for losses (correction factor 2 and 10, respectively). Numbers in brackets give one standard deviation from the original measurement multiplied by the loss correction factor. The two columns can be added up to calculate the total sub-23 nm fraction.

Vehicle	PM mg/km	Total PN (EEPS)			SPN		
		EEPS23 [p/km]	(EEPS10-EEPS23) /EEPS23	(EEPS6-EEPS10) /EEPS23	CPC23 [p/km]	(CPC10-CPC23) /CPC23	(nCNC1-CPC10) /CPC23
DPF_1	0.09	1.2E10	30%	12%	1.1E10	20% ( $\pm 2\%$ )	<det. limit
DPF_2	0.07	7.0E10	14%	3%	6.9E10	20% ( $\pm 18\%$ )	<det. limit
G-PFI_1	0.11	8.1E10	128%	51%	7.7E10	148% (—)	n/a
G-PFI_2	0.25	2.2E11	183%	17%	2.1E11	74% ( $\pm 10\%$ )	0% ( $\pm 10\%$ )
G-DI_1	0.80	1.0E12	32%	14%	1.3E12	50% ( $\pm 4\%$ )	30% ( $\pm 20\%$ )
G-DI_2	1.66	1.4E12	12%	12%	1.4E12	36% ( $\pm 8\%$ )	0% ( $\pm 5\%$ )
Mo_2s	60.1	1.3E13	2%	1%	9.0E12	88% ( $\pm 24\%$ )	150% ( $\pm 40\%$ )
Mo_4s	0.70	1.1E12	34%	5%	4.2E11	142% ( $\pm 34\%$ )	70% ( $\pm 50\%$ )

ambient temperatures, fuel composition, driving style (or test cycle) can have an effect (Maricq et al. 2000; Khalek et al. 2010; Mamakos et al. 2013).

The fraction of sub-23 nm particles of mopeds and motorcycles is typically high. For these technologies, the sampling system can affect the result as the size of the particles is close to or lower than the regulated limit of 23 nm. In addition, effects of pre-history (memory) from the tubing between the motorcycle and the dilution tunnel can affect the results (Maricq et al. 1999). More details can be found in Giechaskiel et al. (2015b).

The conclusion of this study is that the solid sub-23 nm fractions can be significant; however, the sub-23 nm absolute emission levels might be low. For example, G-PFI vehicles are still below the SPN limit even when including the sub-23 nm fraction. Thus, for regulatory purposes the current methodology still captures high emitters for most of the cases (i.e., a vehicle that passes with the 23 nm CPC would also pass with the 10 nm CPC and vice versa). A critical situation would be to have many vehicles in the area between the two dashed lines in Figure 5.

The other finding is that the sub-10 nm percentages are relatively low for G-DI and diesel vehicles. Although this conclusion cannot be extrapolated to other vehicles or technologies (e.g., mopeds showed higher percentage), taken together with high particle losses in the sub-10 nm range and uncertainties of the measurements, it supports the idea of decreasing the lower size to around 10 nm with the current sampling systems, but not lower.

### Sub-23 nm fraction of total particles

The total PN concentrations with sizes  $>23$  nm and the sub-23 nm fractions are presented in Table 2. With the total number, we are here referring to the PN measured without any thermal pre-treatment of the aerosol (i.e., the volatile particles are included). The solid and total number concentrations of larger than 23 nm for cars are comparable within the calibration and experimental uncertainties. For mopeds the difference of solid and total particle emissions larger than 23 nm is 50–100%, indicating a high percentage of volatile particles even above 23 nm. The fractions of total and solid particles below 23 nm are similar for vehicles equipped with DPFs and the G-DI vehicles, indicating a negligible volatile nucleation mode. For the G-PFI vehicles, the sub-23 nm fraction of total particles is higher than the solid particle fraction, indicating a separate nucleation mode. For mopeds, the total sub-23 nm fraction is very low, but as mentioned above, the total concentrations of total and solid particles are different, thus the volatile nucleation mode is larger than 23 nm.

The comparison of the total PN emission with the literature is out of the scope of this article. Nevertheless, the results are in line with results reported by Tzamkiozis et al. (2010), Karavalakis et al. (2015), and Ntziachristos and Galassi (2014). It should be noted though, that the total PN concentrations and the reported fractions between solid and volatile particles should be considered with care: firstly, as mentioned in the introduction, during our calibration measurements we found 20–25% differences between the CPC and the EEPS when checking the instruments with particles larger than 23 nm. This difference was taken into account, but it doesn't mean it's the same for all technologies or concentration levels. Secondly, it is known that the formation of the nucleation mode and its magnitude depend on the dilution conditions (Khalek et al. 1999); thus, measurements from the dilution tunnel with its variable dilution ratio during a test makes it difficult to compare any nucleation mode results with other studies or even with different vehicles of the same lab. Sometimes the tests at the CVS are affected by desorption from the tube between the vehicle and the CVS (Maricq et al. 1999). Finally, the EEPS has a lower size of 5.6 nm, and the contribution of smaller particles is not taken into account in the total concentration or the estimation of the GMD. Some cases worth of mentioning are discussed below.

Figure 6 shows the real-time PN concentration of nCNC (total PN  $>1$  nm) and EEPS (total PN  $>6$  nm and  $>23$  nm), both connected to the CVS at the start of a WMTC cycle for the 4-stroke moped. The nCNC measured downstream from a diluter (dilution 300:1). Concentrations are corrected by the PCRF and dilution of the measurement systems but not the CVS dilution (i.e. concentrations refer to the CVS). The GMD as estimated by the EEPS is also presented in the figure. For comparison, the SPN larger than 23 nm as measured by the

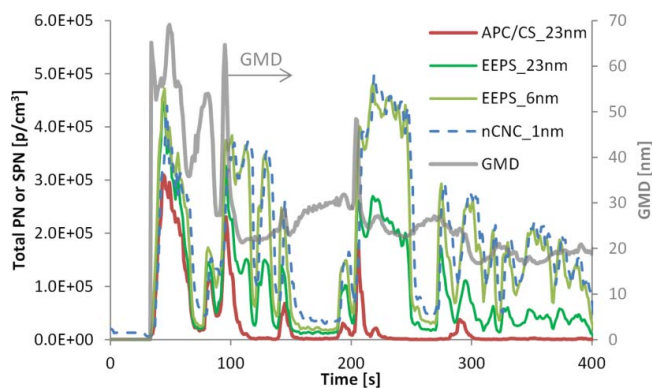


**Figure 6.** Real-time signals of various instruments connected to the CVS with the 4-stroke moped (Mo\_4s). Cold start WMTC. Concentrations refer to the CVS. The Geometric Mean Diameter (GMD) is also shown on the right y-axis.

APC/CS that is also connected to the CVS is presented. At the beginning of the cycle, the GMD is 50–70 nm and all instruments correlate relatively well. After the first 100 s, the GMD decreases, and concentration measured by EEPS (>23 nm) is much higher than the APC/CS, indicating a high number of volatile particles. The agreement between nCNC and EEPS remains good (when using the soot matrix for the EEPS data inversion), suggesting that the nucleation mode is larger than 6 nm. Note that using the original matrix, EEPS and nCNC would have differences of 50% after time 150 s and would lead to the wrong conclusion that there are particles smaller than 6 nm.

Figure 7 compares the nCNC and the EEPS (using the soot matrix) measuring directly from the CVS during an NEDC cycle with the G-PFI\_1 vehicle. The SPN larger than 23 nm and the total PN larger than 23 nm with EEPS are not presented for better readability of the figure as they were very close to the EEPS >6 nm line. The correlation between the instruments is good for the first 1,000 s (note that the nCNC was saturated at  $5 \times 10^5$  p/cm<sup>3</sup> and is calibrated up to  $1 \times 10^5$  p/cm<sup>3</sup>). At the end of the cycle, a big difference is seen, suggesting the formation of a nucleation mode with a GMD smaller than 6 nm. This nucleation mode probably originates from desorption of material in the catalyst and the tubes that connect the vehicle to the CVS during the increase of the exhaust gas temperature (Maricq et al. 1999). Note that in this example the nucleation mode remained at relatively small sizes (majority <6 nm).

This example shows the importance of the lower cut-size of the instruments when determining nucleation mode particles; this is well known from atmospheric studies where a small difference in the cut-point of the CPCs can have a big effect on the result (Sipilä et al. 2010). In addition, investigations of the origins of the

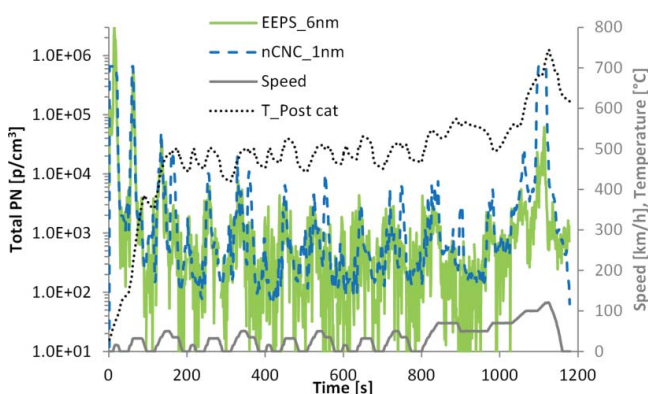


Figure 7. Real-time signals of EEPS and nCNC during an NEDC with the G-PFI vehicle (fuel E5). Both instruments were connected to the CVS. nCNC saturated at  $5 \times 10^5$  p/cm<sup>3</sup>.

nucleation mode need instruments that measure from the formation of the primary cluster (i.e., 1–2 nm). In this size range though we approach the molecules' sizes and particles become indistinguishable from molecules. Considering also the complexity of such measurements, especially sampling systems, they are out of the scope of the regulation.

### Size distributions

Typical size distributions during events of high concentration are presented in Figure 8. All size distributions were taken with the EEPS measuring from the CVS, but they were corrected with the dilution of the CVS, thus the concentrations refer to the tailpipe. Modes of size distributions of vehicles equipped with a DPF were around 60–80 nm, while the modes for gasoline vehicles were around 40–90 nm with a shoulder at the size distribution at around 10 nm in some cases.

Based on the EEPS measurements, the Geometric Mean Diameters (GMD) throughout a test cycle (R47) for the two mopeds with and without thermal pre-treatment are presented in Figure 9. The 2-stroke moped has a GMD of around 150–200 nm at cold start that decreases to 60–130 nm with a warm engine. After thermal pre-treatment of aerosol, the GMD of solid particles is 20–50 nm (75 nm at cold start). The 4-stroke moped has a GMD of 50–130 nm at cold start and 25–40 nm for the rest of the cycle. After thermal pre-treatment of aerosol, the GMD of solid particles is 25 nm, except at accelerations which raise the GMD up to 50 nm. Note that the calculations of small GMDs (<30 nm) would result in smaller GMDs if particles smaller than 6 nm were also counted.

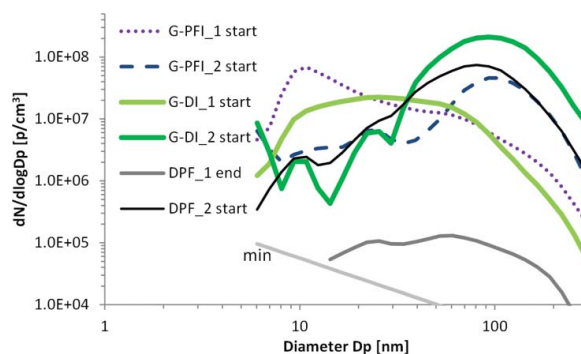
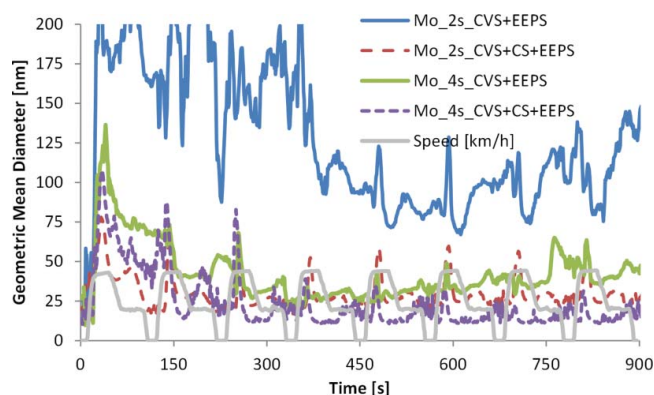


Figure 8. Size distributions measured at the full dilution tunnel (CVS) with an EEPS. Concentrations refer to the tailpipe (i.e., corrected with the CVS dilution of the specific seconds taken). 'Start' refers to the second acceleration and 'end' refers to the high speed part of the cycles. 'Min' refers to the limit of detection of EEPS (multiplied by the dilution at the CVS). The 'Soot' matrix was used for data inversion.





**Figure 9.** Geometric mean diameter throughout R47 test cycles for mopeds as measured by an EEPS directly from the full dilution tunnel (CVS) or through a catalytic stripper (CS). The ‘Soot’ matrix was used.

The size distributions are in good agreement with the literature (references in Giechaskiel et al. 2012 and 2015b).

## Conclusions

Particle emissions of several vehicles were measured, focusing on the sub-23 nm size range. A nano Condensation Nucleus Counter (nCNC) system was used to measure particles of  $>1$  nm in parallel with other Condensation Particle Counters (CPCs) with 50% cut-points at 3 nm, 10 nm, and 23 nm, all connected to various sampling systems using evaporation tubes or catalytic strippers to remove volatiles. It was found that measuring sub-3 nm particle emissions is challenging due to the background of some of the sampling systems. A system had a background of particles with size  $<3$  nm that reached  $2,000$  p/cm<sup>3</sup> (without dilution correction). It was hypothesized that the high background of some systems originated from contamination in the systems from previous tests or from the dilution air. Some contaminants can evaporate from the sampling system walls and re-nucleate before the particle detectors.

An AVL particle counter with a catalytic stripper (APC/CS) and a Dekati ejector-based system with an evaporation tube (EJ/ET) were selected to evaluate the differences between systems with different concepts and particle losses for measuring particle emissions below 23 nm. Penetration at 10 nm of the sampling systems examined was 25% and 75%, respectively, while at 3 nm only the ejector-based system had a  $>15\%$  penetration. It was shown experimentally with a 4-stroke moped that the two sampling systems can have a difference of around 50–150% for the sub-23 nm emissions when the size of particles is also in the 10–20 nm range. Obviously, this difference will depend on the mean size of particles,

and the case examined here is probably the worst one (mean size around 10–15 nm). Thus, future regulations have to better define the (minimum) permitted penetration at the sub-23 nm range in order to minimize the differences between different sampling systems. We believe that penetrations of  $>50\%$  at 10 nm are necessary for reliable measurements.

Another issue for sub-23 nm measurements is the re-nucleation downstream from the thermal pre-treatment unit, the so called volatile artefact. Volatile artefact was evident during the tests of a 2-stroke moped both at the tailpipe and the CVS and gave artificially high emissions of ‘solid’ particles. Volatile artefact was seen in the dilution tunnel with the thermodenuder at low dilutions and even with the catalytic stripper during a cold start of the 2-stroke moped when measuring particles of diameter  $<10$  nm. Based on estimated volatile mass emissions at the CVS, we recommend that the volatile removal efficiency of the system should be checked with a mass of  $1$  mg/m<sup>3</sup> (at the moment, regulation requires  $0.0001$  mg/m<sup>3</sup>).

Based on the measurements of this study with the catalytic stripper-based system (APC/CS), DPF vehicles had a very low sub-23 nm fraction ( $<20\%$ ) over the tested cycles. The G-DI vehicles had a fraction between 35 and 50%. The G-PFI vehicles and mopeds (2-stroke and 4-stroke) had high percentages of sub-23 nm particles ( $>75\%$ ). However, for G-PFIs the emission levels ( $0.7$ – $2.1 \times 10^{11}$  p/km) were below the current limit of  $6 \times 10^{11}$  p/km while for the mopeds they were one order of magnitude higher ( $4$ – $90 \times 10^{11}$  p/km). The fraction of sub-10 nm was difficult to quantify due to the high loss correction factors, but was high only for the mopeds.

Similar sub-23 nm particle fractions were measured for total and solid particle concentrations for passenger cars, with the exception of the G-PFIs where a separate nucleation mode existed. For one G-PFI, during the high speed part of the cycle the nucleation mode had a mean size  $<6$  nm. Regarding mopeds, the sub-23 nm particle fraction was very low and all volatiles were  $>23$  nm.

Size distribution measurements showed that the mode of the DPF vehicles was around 60–80 nm (GMD 50–75 nm), while for the gasoline vehicles it was around 40–90 nm with a small shoulder at the size distribution at around 10 nm (GMD ranging 20–90 nm). For mopeds, the mode (and GMD) was 20–50 nm (after a CS), but in the range of 50–200 nm without a catalytic stripper.

The findings of the study support that a lower limit of around 10 nm for legislative purposes is feasible. The sub-10 nm particle fraction can only be evaluated with systems with better penetration efficiencies and volatile removal efficiencies. In addition, the findings of this study are based on measurements from the dilution

tunnel, and thus the contribution of the tubing between the vehicle and the dilution tunnel at the sub-23 nm particle measurements is to be investigated not only for total particle but even for 'solid' particles.

## Nomenclature

APC	AVL particle counter
CPC	condensation particle counter
CS	catalytic stripper
CVS	constant volume sampler
CVT	continuously variable transmission
DB	dilution bridge
DEG	diethylene glycol
DPF	diesel particulate filter
EEPS	engine exhaust particle sizer
EJ	ejector
ET	evaporation tube
GMD	geometric mean diameter
G-DI	gasoline direct injection
G-PFI	gasoline port fuel injection
NEDC	new European driving cycle
nCNC	nano condensation nucleus counter
PM	particulate matter
PMP	particle measurement program
PN	particle number
PSM	particle size magnifier
R47	Regulation 47 (UNECE)
SPN	solid particle number
TD	thermodenuder
VPR	volatile particle remover
WMTC	World Harmonized Motorcycle Transient Cycle
UNECE	United Nations–Economic Commission for Europe

## Disclaimer

The views expressed here are those of the authors and may not be considered as the official position of the European Commission.

## References

Alanen, J., Saukko, E., Lehtoranta, K., Murtonen, T., Timonen, H., Hillamo, R., Karjalainen, P., Kuuluvainen, H., Harra, J., Keskinen, J., and Rönkkö, T. (2015). The Formation and Physical Properties of the particle Emissions from a Natural Gas Engine. *Fuel*, 162:155–161. doi:10.1016/j.fuel.2015.09.003

Amanatidis, S., Ntziachristos, L., Giechaskiel, B., Bergmann, A., and Samaras, Z. (2014). Impact of Selective Catalytic Reduction on Exhaust Particle Formation Over Excess Ammonia Events. *Environ. Sci. Technol.*, 48:11527–11534.

Amanatidis, S., Ntziachristos, L., Giechaskiel, B., Katsaounis, D., Samaras, Z., and Bergmann, A. (2012). Evaluation of an Oxidation Catalyst ("Catalytic Stripper") in Eliminating Volatile Material from Combustion Aerosol. *J. Aerosol Sci.*, 57:144–155. doi:10.1016/j.jaerosci.2012.12.001

Andersson, J., Giechaskiel, B., Munoz-Bueno, R., and Dilara, P. (2007). *Particle measurement programme (PMP): Light-duty inter-laboratory correlation exercise (ILCE LD)-Final report (EUR 22775 EN) GRPE-54-08-Rev.1*, <http://www.unece.org/trans/main/wp29/wp29wgs/wp29grpe/grpeinf54.html>

Braisher, M., Stone, R., and Price, P. (2010). Particle Number Emissions from a Range of European Vehicles. SAE Technical Paper 2010-01-0786.

Ciuffo, B., Marotta, A., Tutuiianu, M., Fontaras, G., Pavlovic, J., Tsiakmakis, S., Anagnostopoulos, K., Serra, S., and Zacharof, . (2015). N. Development of the World-wide Harmonized Test Procedure for Light-Duty Vehicles. Pathway for its Implementation into EU legislation. *Transportation Research Records. J. Trans. Res. Board*, 2503:110–118.

D'Anna, A. (2009). Combustion-formed Nanoparticles. *Proc. Combust. Inst.*, 32:593–613.

Dieselnet. (2016). Emission Test Cycles. <https://www.dieselnet.com/standards/cycles/>

Fierz, M., Vernooij, M., and Burtscher, H. (2007). An Improved Low-Flow Thermodenuder. *J. Aerosol Sci.*, 38:1163–1168. <http://dx.doi.org/10.1016/j.jaerosci.2007.08.006>

Gidney, J., Twigg, M., and Kittelson, D. (2010). Effect of Organometallic Fuel Additives on Nanoparticle Emissions from a Gasoline Passenger Car. *Environ. Sci. Technol.*, 44:2562–2569.

Giechaskiel, B., and Martini, G. (2014). Engine Exhaust Solid Sub-23 nm Particles: II. Feasibility Study for Particle Number Measurement Systems. *SAE Int. J. Fuels Lubr.*, 7:935–949. doi: 10.4271/2014-01-2832. doi:10.4271/2014-01-2832

Giechaskiel, B., and Martini, G. (2015). PMP-37-02 Raw Exhaust PN Counting. Presentation for the PMP group. Available at: <https://www2.unece.org/wiki/display/trans/PMP+37th+Session>

Giechaskiel, B., Carriero, M., Martini, G., Krasenbrink, A., and Scheder, D. (2009). Calibration and Validation of Various Commercial Particle Number Measurement Systems. *SAE Int. J. Fuels Lubr.*, 2(1):512–530. doi:10.4271/2009-01-1115

Giechaskiel, B., Cresnoverh, M., Jörgl, H., and Bergmann, A. (2010). Calibration and Accuracy of a Particle Number Measurement System. *Meas. Sci. Technol.*, 21(4):045102. doi: 10.1088/0957-0233/21/4/045102

Giechaskiel, B., Dilara, P., and Andersson, J. (2008). Particle Measurement Programme (PMP) Light-Duty Inter-Laboratory Exercise: Repeatability and Reproducibility of the Particle Number Method. *Aerosol Sci. Technol.*, 42:528–543. doi:10.1080/02786820802220241

Giechaskiel, B., Mamakos, A., Andersson, J., Dilara, P., Martini, G., Schindler, W., and Bergmann, A. (2012). Measurement of Automotive Non-Volatile Particle Number Emissions within the European Legislative Framework: A Review. *Aerosol Sci. Technol.*, 46:719–749.

Giechaskiel, B., Manfredi, U., and Martini, G. (2014). Engine Exhaust Solid Sub-23 nm Particles: I. Literature Survey. *SAE Int. J. Fuels Lubr.*, 7:950–964. doi: 10.4271/2014-01-2834

- Giechaskiel, B., Riccobono, F., and Bonnel, P. (2015a). *Feasibility study on the extension of the real driving emissions (RDE) procedure to particle number (PN): Chassis dynamometer evaluation of portable emission measurement systems (PEMS) to measure particle number (PN) concentration: Phase II. JRC report*, Ispra, Italy. ISBN 978-92-79-51003-8, 10.2790/74218 <http://publications.jrc.ec.europa.eu/repository/handle/JRC97357>
- Giechaskiel, B., Zardini, A., and Martini, G. (2015b). Particle Emission Measurements from L-Category Vehicles. *SAE Int. J. Engines*, 8(5):2322–2337. doi: 10.4271/2015-24-2512
- Giechaskiel, B., Riccobono, F., Mendoza, P., and Grigoratos, T. (2016). Particle Number (PN) - Portable Emissions Measurement Systems (PEMS): Heavy Duty Vehicles Evaluation Phase at the Joint Research Centre (JRC). *JRC scientific report EUR 28256 EN*. doi: 10.2788/052796
- Gormley, P. G., and Kennedy, M. (1949). Diffusion from a Stream Flowing Through a Cylindrical Tube. *Proc. Sci. Technol.*, 12:163–169.
- GTR15. (2016). Global Technical Regulation No. 15. Worldwide Harmonized Light Vehicles Test Procedure. UNECE, Geneva, Switzerland, 2016; [http://www.unece.org/fileadmin/DAM/trans/doc/2016/wp29grpe/ECE-TRANS-WP29-GRPE-2016-03e\\_clean.pdf](http://www.unece.org/fileadmin/DAM/trans/doc/2016/wp29grpe/ECE-TRANS-WP29-GRPE-2016-03e_clean.pdf)
- Heikkilä, J., Rönkkö, T., Lähde, T., Lemmetty, M., Arffman, A., Virtanen, A., Keskinen, J., Pirjola, L., and Rothe, D. (2009). Effect of Open Channel Filter on Particle Emissions of Modern Diesel Engine. *J. Air Waste Manag. Assoc.*, 59(10):1148–1154.
- Herner, J., Robertson, W., and Ayala, A. (2007). Investigation of Ultrafine Particle Number Measurements from a Clean Diesel Truck Using the European PMP Protocol, SAE Technical Paper 2007-01-1114.
- Horizon. (2020). *GV-02-2016 Technologies for low emission light duty powertrains*, <https://ec.europa.eu/research/participants/portal/desktop/en/opportunities/h2020/topics/2064-gv-02-2016.html>
- Johnson, K., Durbin, T., Jung, H., Chaudhary, A., Cocker, D., Herner, J., Robertson, W., Huai, T., Ayala, A., and Kittelson, D. (2009). Evaluation of the European PMP Methodologies During On-Road and Chassis Dynamometer Testing for DPF Equipped Heavy-Duty Diesel Vehicles. *Aerosol Sci. Technol.*, 43(10):962–969.
- Kangasluoma, J., Kuang, C., Wimmer, D., Rissanen, M. P., Lehtipalo, K., Ehn, M., Worsnop, D. R., Wang, J., Kulmala, M., and Petäjä, T. (2014). Sub-3 nm Particle Size and Composition Dependent Response of a Nano-CPC Battery. *Atmos. Meas. Tech.*, 7:689–700.
- Karavalakis, G., Short, D., Vu, A., Russell, R., Asa-Awuku, A., and Durbin, T. (2015). Complete Assessment of the Emissions Performance of Ethanol Blends and Iso-Butanol Blends from a Fleet of Nine PFI and GDI Vehicles. SAE Technical Paper 2015-01-0957. doi:10.4271/2015-01-0957
- Karjalainen, P., Pirjola, L., Heikkilä, J., Lähde, T., Tzamkiozis, T., Ntziachristos, L., Keskinen, J., and Rönkkö, T. (2014). Exhaust particles of modern gasoline vehicles: A laboratory and an on-road study. *Atmos. Environ.*, 97:262–270.
- Karjalainen, P., Pirjola, L., Heikkilä, J., Lähde, T., Tzamkiozis, T., Ntziachristos, L., Keskinen, J., and Rönkkö, T. (2014). Exhaust Particles of Modern Gasoline Vehicles: A Laboratory and an On-Road Study. *Atmos. Environ.*, 97:262–270. doi:10.1016/j.atmosenv.2014.08.025
- Keskinen, J., and Rönkkö, T. (2010). Can Real-World Diesel Exhaust Particle Size Distribution be Reproduced in the Laboratory? A Critical Review. *J. Air Waste Manag. Assoc.*, 60(10):1245–1255. doi:10.3155/1047-3289.60.10.1245
- Khalek, I. (2007). Sampling System for Solid and Volatile Exhaust Particle Size, Number, and Mass Emissions. SAE Technical Paper 2007-01-0307. doi:10.4271/2007-01-0307
- Khalek, I., and Kittelson, D. (1995). Real Time Measurement of Volatile and Solid Exhaust Particles Using a Catalytic Stripper. SAE Technical Paper 950236. doi:10.4271/950236
- Khalek, I., Bougher, T., and Jetter, J. (2010). Particle Emissions from a 2009 Gasoline Direct Injection Engine Using Different Commercially Available Fuels. *SAE Int. J. Fuels Lubr.*, 3(2):623–637. doi:10.4271/2010-01-2117
- Khalek, I., Kittelson, D., and Brear, F. (1999). The Influence of Dilution Conditions on Diesel Exhaust Particle Size Distribution Measurements. SAE Technical Paper 1999-01-1142.
- Kim, J., Choi, K., Myung, C., Lee, Y., and Park, S. (2013). Comparative Investigation of Regulated Emissions and Nano-Particle Characteristics of Light Duty Vehicles Using Various Fuels for the FTP-75 and the NEDC Mode. *Fuel*, 106:335–343.
- Kittelson, D. (1998). Engines and Nanoparticles: A Review. *J. Aerosol Sci.*, 29:575–588.
- Kittelson, D., Watts, W., and Johnson, J. (2006). On-Road and Laboratory Evaluation of Combustion Aerosols. Part1: Summary of Diesel Engine Results. *J. Aerosol Sci.*, 37:913–930.
- Ku, B.K., and Maynard, A.D. (2006). Generation and Investigation of Airborne Silver Nanoparticles with Specific Size and Morphology by Homogeneous Nucleation, Coagulation and Sintering. *J. Aerosol Sci.*, 37:452–470.
- Kumar, P., Morawska, L., Birmili, W., Paasonen, P., Hu, M., Kulmala, M., Harrison, R., Norford, L., and Britter, R. (2014). Ultrafine Particles in Cities. *Environ.Int.*, 66:1–10. doi:10.1016/j.envint.2014.01.013
- Lähde, T., Rönkkö, T., Virtanen, A., Schuck, T., Pirjola, L., Hämeri, K., Kulmala, M., Arnold, F., Rothe, D., and Keskinen, J. (2009). Heavy-Duty Diesel Engine Exhaust Aerosol Particle and Ion Measurements. *Environ. Sci. Technol.*, 43:163–168.
- Lehtipalo, K. et al. (2016). The Effect of Acid-Base Clustering and Ions on the Growth of Atmospheric Nano-Particles. *Nature Commun.*, 7:11594.
- Liu, G., Vasys, V., Dettmann, M., Schauer, J., Kittelson, D., and Swanson, J. (2009). Comparison of Strategies for the Measurement of Mass Emissions from Diesel Engines Emitting Ultra-Low Levels of Particulate Matter. *Aerosol Sci. Technol.*, 43:1142–1152.
- Lobo, P., Durdina, L., Smallwood, G., Rindlisbacher, T., Siegerist, F., Black, E., Yu, Z., Mensah, A., Hagen, D., Miake-Lye, R., Thomson, K., Brem, B., Corbin, J., Abegglen, M., Sierau, B., Whitefield, P., and Wang, J. (2015). Measurement of Aircraft Engine Non-Volatile PM emissions: results of the aviation-particle regulatory instrumentation demonstration experiment (A-PRIDE) 4 campaign. *Aerosol Sci. Technol.*, 49(7):472–484. doi: 10.1080/02786826.2015.1047012
- Mamakos, A., Dardiotis, C., and Martini, G. (2012). Assessment of Particle Number Limits for Petrol Vehicles. *EU Report 25592*. Available at: <http://publications.jrc.ec.europa.eu/repository/bitstream/JRC76849/lbna25592enn.pdf>
- Mamakos, A., Giechaskiel, B., and Drossinos, Y. (2013). Experimental and Theoretical Investigation of the Effect of the



- Calibration Aerosol Material on the Counting Efficiencies of TSI 3790 Condensation Particle Counters. *Aerosol Sci. Technol.*, 47(1):11–21.
- Mamakos, A., Giorgio, M., Alessandro, M., and Manfredi, U. (2013). Assessment of Different Technical Options in Reducing Particle Emissions from Gasoline Direct Injection Vehicles. *J. Aerosol Sci.*, 63:115–125.
- Maricq, M., Chase, R., Podsiadlik, D., and Vogt, R. (1999). Vehicle Exhaust Particle Size Distributions: A Comparison of Tailpipe and Dilution Tunnel Measurements. SAE Technical Paper 1999-01-1461.
- Maricq, M., Munoz, R., Yang, J., and Anderson, R. (2000). Sooting Tendencies in an Air-Forced Direct Injection Spark-Ignition (DISI) Engine. SAE Technical Paper 2000-01-0255, doi:10.4271/2000-01-0255
- Maricq, M., Chase, R., Xu, N., Podsiadlik, D. (2002). The Effects of the Catalytic Converter and Fuel Sulfur Level on Motor Vehicle Particulate Matter Emissions: Gasoline Vehicles. *Environ. Sci. Technol.*, 36:276–282.
- Mayer, A., Czerwinski, J., Kasper, M., Ulrich, A., and Mooney, J. (2012). Metal Oxide Particle Emissions from Diesel and Petrol Engines. SAE Technical Paper 2012-01-0841. doi:10.4271/2012-01-0841
- Mayer, A., Ulrich, A., Czerwinski, J., and Mooney, J. (2010). Metal-Oxide Particles in Combustion Engine Exhaust. SAE 2010-01-0792. doi:10.4271/2010-01-0792
- Mendes, L., Eleftheriadis, K., and Biskos, K. (2016). Performance Comparison of Two Thermodenuders in Volatility Tandem DMA Measurements. *J. Aerosol Sci.*, 92:38–52.
- Morawska, L., Ristovski, Z., Jayaratne, E., Keogh, D., and Ling, X. (2008). Ambient Nano and Ultrafine Particles from Motor Vehicle Emissions: Characteristics, Ambient Processing and Implications on Human Exposure. *Atmos. Environ.*, 42:8113–8138. doi:10.1016/j.atmosenv.2008.07.050
- Ntziachristos, L., Amanatidis, S., Samaras, Z., Giechaskiel, B., and Bergmann, A. (2013). Use of a Catalytic Stripper as an Alternative to the Original PMP Measurement Protocol. *SAE Int. J. Fuels Lubr.*, 6(2):532–541. doi:10.4271/2013-01-1563
- Ntziachristos, L., and Galassi, M. (2014). Emission Factors for New and Upcoming Technologies in Road Transport. *JRC Report 26952*, Ispra.
- Ntziachristos, L., Giechaskiel, B., Pistikopoulos, P., Fysikas, E., and Samaras, Z. (2003). Particle Emissions Characteristics of Different On-Road Vehicles. SAE technical paper 2003-01-1888.
- Oberdörster, G., Sharp, Z., Atudorei, V., Elder, A., Gelein, R., Kreyling, W., and Cox, C. (2004). Translocation of Inhaled Ultrafine Particles to the Brain. *Inhal Toxicol.*, 16(6–7):437–45.
- Otsuki, Y., Takeda, K., Haruta, K., and Mori, N. (2014). A Solid Particle Number Measurement System Including Nanoparticles Smaller Than 23 Nanometers. SAE Technical Paper 2014-01-1604. doi:10.4271/2014-01-1604
- Regulation 83. (2015). United Nations – Economic Commissions for Europe, Regulation no. 83, Revision 5, 22 Jan 2015, Uniform provisions concerning the approval of vehicles with regard to the emissions of pollutants according to engine fuel requirements.
- Rönkkö, T., Pirjola, L., Ntziachristos, L., Heikkilä, J., Karjalainen, P., Hillamo, R., and Keskinen, J. (2014). Vehicle Engines Produce Exhaust Nanoparticles Even When not Fueled. *Environ. Sci. Technol.*, 48:2043–2050. doi: 10.1021/es405687m
- Rönkkö, T., Virtanen, A., Kannosto, J., Keskinen, J., Lappi, M., and Pirjola, L. (2007). Nucleation Mode Particles with a Nonvolatile Core in the Exhaust of a Heavy-Duty Diesel Vehicle. *Environ. Sci. Technol.*, 41:6384–6389.
- Rönkkö, T., Virtanen, A., Kannosto, J., Keskinen, J., Lappi, M., and Pirjola, L. (2007). Nucleation Mode Particles with a Nonvolatile Core in the Exhaust of a Heavy-Duty Diesel Vehicle. *Environ. Sci. Technol.*, 41:6384–6389. doi: 10.1021/es0705339
- Sipilä, M., Berndt, T., Petäjä, T., Brus, D., Vanhanen, J., Stratmann, F., Patokoski, J., Mauldin, R. L. III, Hyvärinen, A.-P., Lihavainen, H., and Kulmala, M. (2010). The Role of Sulfuric Acid in Atmospheric Nucleation. *Science*, 327(5980):1243–1246. doi:10.1126/science.1180315
- Swanson, J., and Kittelson, D. (2010). Evaluation of Thermal Denuder and Catalytic Stripper Methods for Solid Particle Measurements. *J. Aerosol Sci.*, 41:1113–1122.
- Swanson, J., Kittelson, D., Giechaskiel, B., Bergmann, A., and Twigg, M. (2013). A Miniature Catalytic Stripper for Particles Less Than 23 nm. *SAE Int. J. Fuels Lubr.*, 6(2):542–551. doi:10.4271/2013-01-1570
- Swanson, J., Kittelson, D., Watts, W., Gladis, D., and Twigg, M. (2009). Influence of Storage and Release on Particle Emissions from New and Used CRTs. *Atmos. Environ.*, 43:3998–4004.
- Szybist, J., Youngquist, A., Barone, T., Storey, J., Moore, W., Foster, M., and Confer, K. (2011). Ethanol Blends and Engine Operating Strategy Effects on Light-Duty Spark-Ignition Engine Particle Emissions. *Energy Fuels*, 25(11):4977–4985.
- Tuch, T., Weinhold, K., Merkel, M., Nowak, A., Klein, T., Quincey, P., Stolzenburg, M., and Wiedensohler, A. (2016). Dependence of CPC Cut-Off Diameter on Particle Morphology and Other Factors. *Aerosol Sci. Technol.*, 50(4):331–338, doi: 10.1080/02786826.2016.1152351
- Tzankiozis, T., Ntziachristos, L., and Samaras, Z. (2010). Diesel Passenger Car PM Emissions: From Euro 1 to Euro 4 with Particle Filter. *Atmos. Environ.*, 44:909–916.
- Vanhanen, J., Mikkilä, J., Lehtipalo, K., Sipilä, M., Manninen, H.E., Siivola, E., Petäjä, T., and Kulmala, M. (2011). Particle Size Magnifier for Nano-CN Detection. *Aerosol Sci. Technol.*, 45:533–542.
- Wang, X.L., Grose, M.A., Avenido, A., Stolzenburg, M.R., Caldwell, R., Osmondson, B.L., Chow, J.C., and Watson, J.G. (2016). Improvement of Engine Exhaust Particle Sizer (EEPS) Size Distribution Measurement - I. Algorithm and Applications to Compact Aerosols. *J. Aerosol Sci.*, 92:95–108.
- Xue, J., Li, Y., Wang, X., Durbin, T., Johnson, K., Karavalakis, G., Asa-Awuku, A., Villela, M., Quiros, D., Hu, S., Huai, T., Ayala, A., and Jung, H. (2015). Comparison of Vehicle Exhaust Particle Size Distributions Measured by SMPS and EEPS During Steady-State Conditions. *Aerosol Sci. Technol.*, 49(10):984–996, doi: 10.1080/02786826.2015.1088146
- Yamada, H., Funato, K., and Sakurai, H. (2015). Application of the PMP Methodology to the Measurement of Sub-23 nm Solid Particles: Calibration Procedures, Experimental Uncertainties, and Data Correction Methods. *J. Aerosol Sci.*, 88:58–71. doi: 10.1016/j.jaerosci.2015.06.002
- Zheng, A., Durbin, T., Xue, J., Johnson, K., Li, Y., Hu, S., Huai, T., Ayala, A., Kittelson, D., and Jung, H. (2014). Comparison of



- Particle Mass and Solid Particle Number (SPN) Emissions from a Heavy-Duty Diesel Vehicle Under On-Road Driving Conditions and a Standard Testing Cycle. *Environ. Sci. Technol.*, 48:1779–1786. dx.doi.org/10.1021/es403578b
- Zheng, Z., Durbin, T., Karavalakis, G., Johnson, K., Chaudhary, A., Cocker, D., III; Herner, J., Robertson, W., Huai, T., Ayala, A., Kittelson, D., and Jung, H. (2012). Nature of Sub-23 nm Particles in the Solid Particle Measurement Method: A Real Time Data Perspective. *Aerosol Sci. Technol.*, 46 (7):886–896. doi: 10.1080/02786826.2012.679167
- Zheng, Z., Durbin, T., Karavalakis, G., Johnson, K., Chaudhary, A., Cocker III, D., Herner, J., Robertson, W., Ayala, A., Kittelson, D., and Jung, H. (2012). Nature of Sub-23-nm Particles Downstream of the European Particle Measurement Programme (PMP)-Compliant System: A Real Time Perspective. *Aerosol Sci. Technol.*, 46:886–896.
- Zheng, Z., Johnson, K., Liu, Z., Durbin, T., Hu, S., Huai, T., Kittelson, D., and Jung, H. (2011). Investigation of Solid Particle Number Measurement: Existence and Nature of Sub-23 nm Particles Under PMP Methodology. *J. Aerosol Sci.*, 42(12):883–897.
- Zhu, R., Hu, J., Bao, X., He, L., Lai, Y., Zu, L., Li, Y., and Su, S. (2016). Tailpipe Emissions from Gasoline Direct Injection (GDI) and Port Fuel Injection (PFI) Vehicles at Both Low and High Ambient Temperatures. *Environ. Pollut.*, 216:223–234.